Supplementary materials

Antiferromagnetic ordering in cobalt(II) and nickel(II) 1D coordination polymers with dithioamide of 1,3-benzenedicarboxylic acid

Anton S. Lytvynenko,[a] Sergey V. Kolotilov,[a,b] Olivier Cador,[b] Stéphane Golhen,[b] Lahcène Ouahab[b]* and Vitaly V. Pavlishchuk[a]*

[a] *L. V. Pisarzhevskii Institute of Physical Chemistry of the National Academy of Sciences of the Ukraine, Prospekt Nauki 31, Kiev, 03028, Ukraine, tel. +38 (0)44 525 42 28, fax +38 (0)44 525 62 16, e-mail: shchuk@inphyschem-nas.kiev.ua*

[b] *Equipe Organométalliques et Matériaux Moléculaires, Sciences Chimiques de Rennes, UMR UR1-CNRS 6226, Université de Rennes 1, Campus de Beaulieu, 35042 Rennes cedex, France, tel. +33 (0)2 23 23 56 59, fax +33 (0)2 23 23 68 40, e-mail: lahcene.ouahab@univ-rennes1.fr*

Synthesis of dithioamide of 1,3-benzenedicarboxylic acid (m-dtab). 2.56 g of 1,3-dicyanobenzene was suspended in a mixture of triethylamine (9 mL) and ethanol (24 mL). The mixture was cooled on ice and hydrogen sulfide was slowly bubbled (approximately 1 bubble per second) into the mixture until complete change of suspension's color from white to yellow (4 – 6 hours). Solvents were removed in vacuum, and dry residue was dissolved in 50 mL of DMF, the solution filtered and then diluted with 100 mL of water. Light-yellow precipitate was filtered, washed with water and dried at 150 ºC. Anal. Calcd. for $C_8H_{8.4}N_2S_2O_{0.2}$: C, 48.1; H, 4.21; N, 14,0. Found: C, 47.9; H, 3.96; N, 14.1%. ^{1}H-NMR (DMSO-d_6), δ(ppm): 7.43 t (1H, H5 of aromatic ring), 7.93 d (2H, H4 and H6 of aromatic ring, J_{H4-H5} = 7.75 Hz), 8.29 s (1H, H2 of aromatic ring), 9.55 s (2H, N–H), 9.95 s (2H, N–H). H-atoms have the labels of positions in aromatic ring, determined by IUPAC rules. The signal of -NH_2 group is

split into two components due to hindrance of rotation of NH_2 group around C–N bond. IR, cm^{-1}: ν^{N-H} 3280 (medium), $\nu^{(Thioamide\ I)}$ 1630 (strong).

Details of DFT calculations.

Geometries

The geometry of **1**, used for DFT calculations, was taken from crystallographic data. For calculations of bond orders endless chain of **1** was cut up to $Co(m\text{-}dtab)_2Cl_2$ particle. For calculations of exchange integrals through different pathways (see the main text) in **1**, structure was cut in another ways (*vide infra*).

The geometries of **m-dtab** and **m-phthalateH$_2$**, used for DFT calculations, were obtained by geometry optimization with redundant internal coordinates, as implemented in ORCA. Closed-shell Kohn-Sham formalism (RKS) with hybrid B3LYP[1a-b] (Becke type three parameter exchange,[1a,c] Lee-Yang-Parr correlation,[2] Vosko-Wilk-Nusair VWN-5 free electron gas parametrization[3] for LDA part, fraction of HF exchange – 0.2, scaling of DF-GGA exchange – 0.72, scaling of DF-GGA correlation – 0.81, scaling of LDA correlation – 1.0, with default empirical parameters X-alpha = 2/3; Becke's β = 0.00420) functional and Ahlrichs def2-TZVP basis set[4] (triple-ζ valence basis with polarization functions from Turbomole library[5]) were used in the calculation. The resolution of the identity[6] (RI) and chain-of-spheres (COSX – for treatments of Hartree-Fock exchange part)[7] approximations were used during the calculations to speed up the self-consistent field convergence. The auxiliary basis sets used with RI approximation were built automatically by ORCA. Ahlrichs basis sets were chosen because they were calibrated and validated using extensive tests with more than 300 molecules, including almost all elements in their most common oxidation states[4] and include auxiliary basis sets for RI-DFT and are supposed to be the most efficient in this case.[8] To improve the quality of results the SCF converged tolerance was tightened to $\Delta E \leq 10^{-9}$ E_h and $\Delta E_{1\text{-electron}} \leq 10^{-6}$ E_h (using "VeryTightSCF" keyword). An integration grid was enlarged to Lebedev 302 points[9] one (using "Grid4" keyword). Building of the final grid was turned off. No constrains were applied. RMS gradient tolerance was tightened to 10^{-6} a.u./bohr (other

tolerances, *i.e.* energy change, maximal gradient, maximal step and RMS step, were controlled by ORCA's keyword "TightOpt"). Grimme's semiempirical Van der Waals correction[10] was applied, as implemented in ORCA.

The geometry of **[Co(m-phthalate)(Im)$_2$]$_n$,**[11] used for DFT calculations, was taken from published crystallographic data (CCDC 613933). The infinite chain was cut up to **Co(m-phthalateH)$_2$(Im)$_2$** block, (**m-phthalate**)$^{2-}$ ligands where terminated by hydrogen atoms. Positions of these hydrogens were optimized similar to **m-dtab** and **m-phthalateH$_2$**, but the positions of all another atoms were frozen, spin-unrestricted Kohn-Sham formalism (for S = 3/2) was used and Ahlrichs def2-SVP[4] (double-ζ valence basis set with polarization functions from Turbomole library[5]) was assigned to all atoms except the atoms of terminating carboxyl groups (def2-TZVP was assigned to these atoms). All tolerances, *i.e.* RMS gradient, energy change, maximal gradient, maximal step and RMS step, were controlled by ORCA's keyword "TightOpt".

Images of the geometries, used for the calculations, were rendered using Avogadro package.[12]

Bond orders

Bond orders of **m-dtab**, **m-phthalateH$_2$**, **Co(m-dtab)$_2$Cl$_2$** and **Co(m-phthalate)$_2$Im$_2$** were determined after Mayer[13] using the results of single point calculations. Hybrid B3LYP (*vide supra*) functional and Ahlrichs def2-TZVP basis set[4] were used in the calculation. The resolution of the identity[6] (RI) and chain-of-spheres (COSX – for treatments of Hartree-Fock exchange part)[7] approximations were used. The auxiliary basis sets used with RI approximation were built automatically by ORCA. The SCF converged tolerance was tightened to $\Delta E \leq 10^{-9}$ E_h and $\Delta E_{1\text{-electron}} \leq 10^{-6}$ E_h (using "VeryTightSCF" keyword). An integration grid was enlarged to Lebedev 302 points[9] one (using "Grid4" keyword). Building of the final grid was turned off. The results of this calculation were used to build explicit plots of **m-dtab** orbitals (Fig. S1-S2).

Exchange integrals

For calculation of exchange integrals the endless 3D structures of **1** was cut in order to get the minimal geometries, that include appropriate pathways (See Fig. S5–S8). The calculations were provided using Broken Symmetry DFT approach. SCF of the dinuclear species was first converged to high spin state (S = 3, M_s = 3), then they were reconverged to broken symmetry state (S = 3, M_s = 0). The differences between the obtained energies were used to find values of Heisenberg-Dirac-van Vleck model exchange ($H = -2JS_iS_j$, see text). A few exchange-corellation functionals (GGA BP (Becke '88 exchange,[1c] Perdew '86 correlation[14]), meta-GGA TPSS[15] and hybrid B3LYP) and a few basis sets were used in these calculations (see text and Table S2 and S3) for comparison. The resolution of the identity[6] (RI) approximation was used (but HF exchange was treated exactly, because COSX approximations gives an error with order of 1 cm^{-1} [7]). The auxiliary basis sets used with RI approximation were built automatically by ORCA. The SCF converged tolerance was tightened to $\Delta E \leq 10^{-9}$ E_h and $\Delta E_{1\text{-electron}} \leq 10^{-6}$ E_h (using "VeryTightSCF" keyword). An integration grid was enlarged to Lebedev 434 points[9] one (using "Grid5" keyword). Building of the final grid was turned off.

Similar procedures were employed for calculation of exchange integrals in **2**.

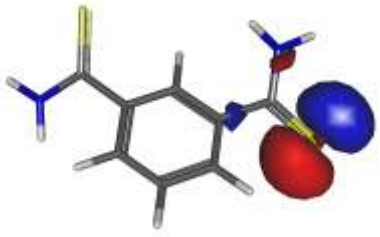

Fig. S1. Plot of HOMO of **m-dtab**. Blue surface refers to positive sign of the wavefunction, red to negative. Calculation shows that equivalent orbital based on another S atom has slightly lower energy.

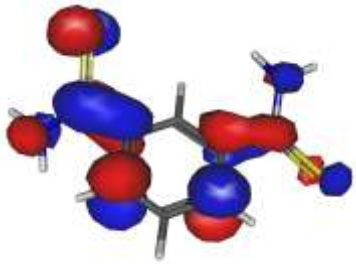

Fig. S2. Plot of LUMO of **m-dtab**. Blue surface refers to positive sign of the wavefunction, red to negative.

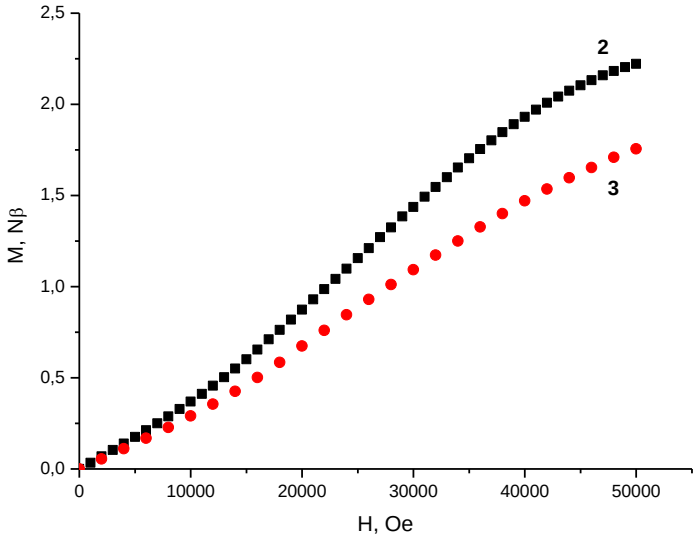

Fig. S3. Magnetization vs. field for **2** and **3** at 2 K.

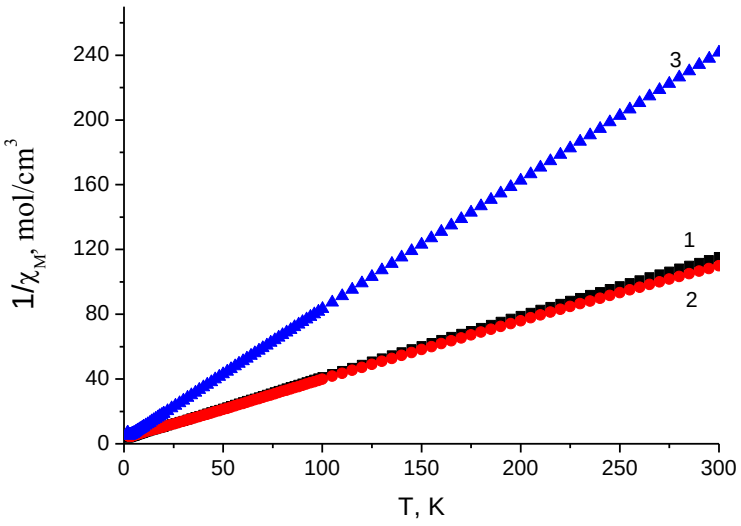

Fig. S4. Plots of $1/\chi$ vs. T for **1** - **3**.

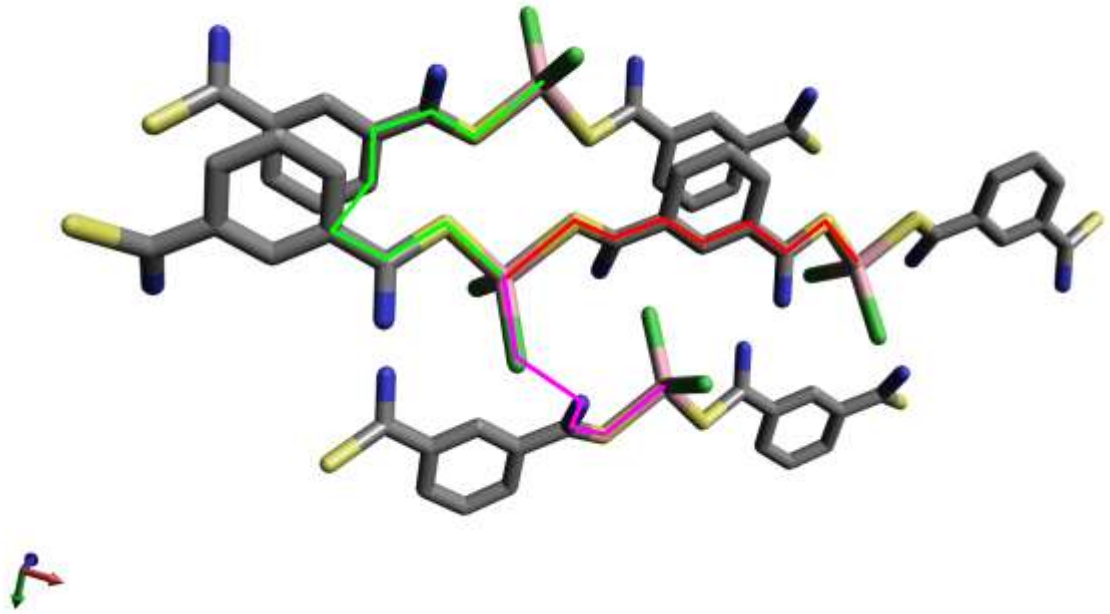

Fig. S5. Exchange pathways in **1**: via bridge (red), via hydrogen bond (magenta) and via π-stacking (green).

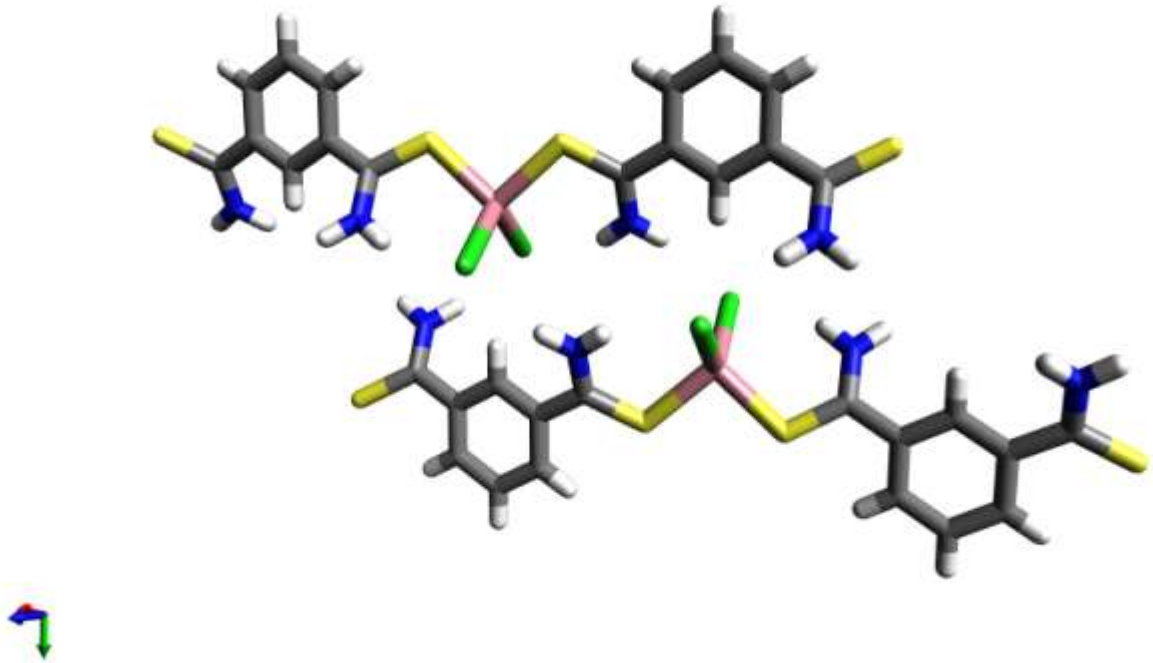

Fig. S6. Geometry of **1** built for calculation of exchange via hydrogen bond.

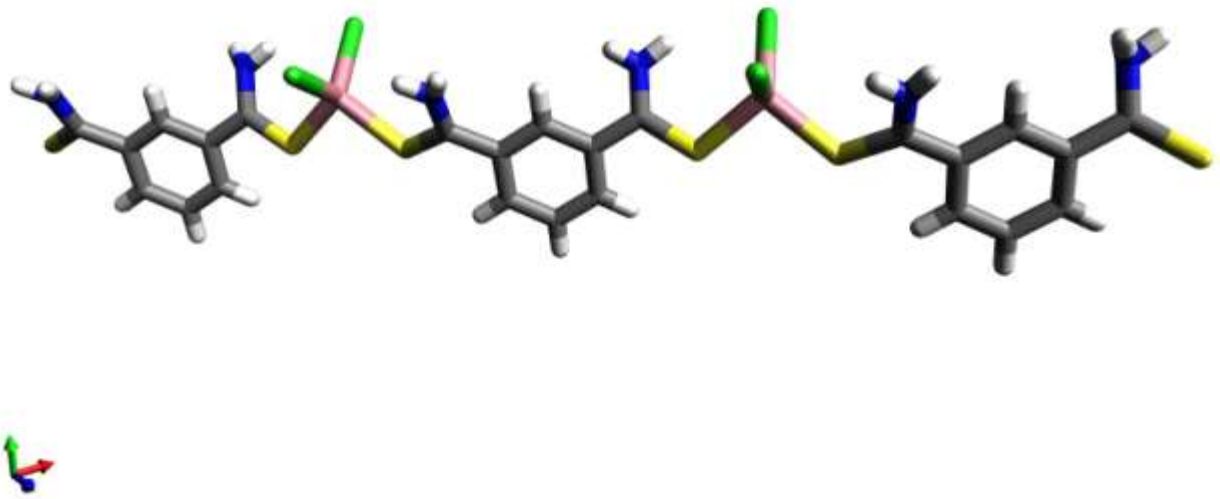

Fig. S7. Geometry of **1** built for calculation of exchange via bridge.

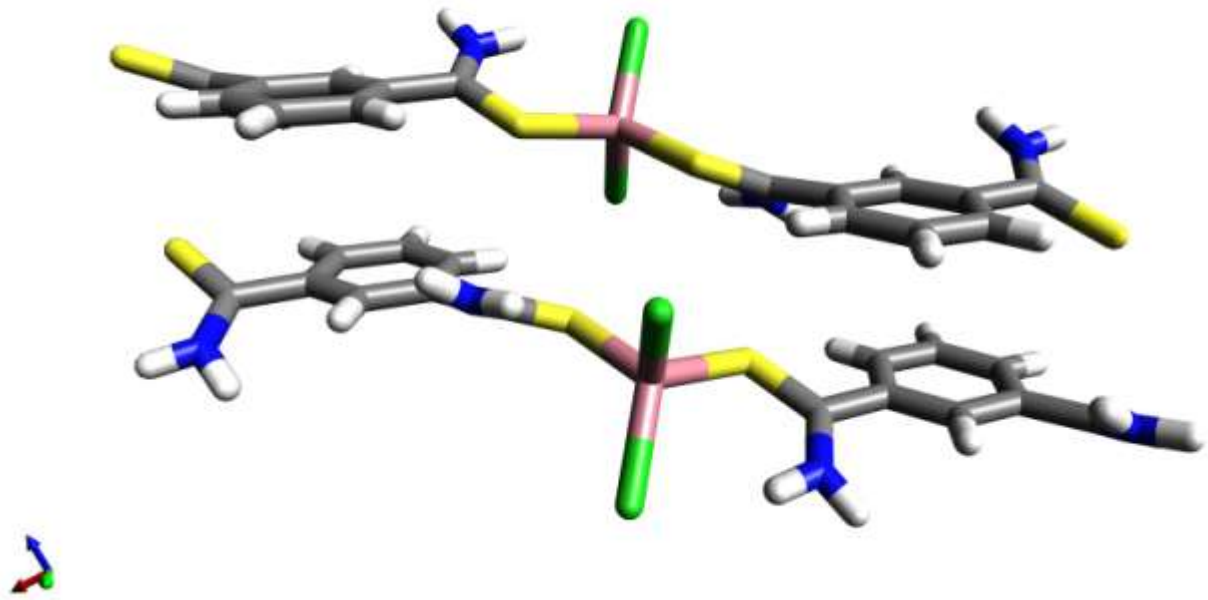

Fig. S8. Geometry of **1** built for calculation of exchange via stacking.

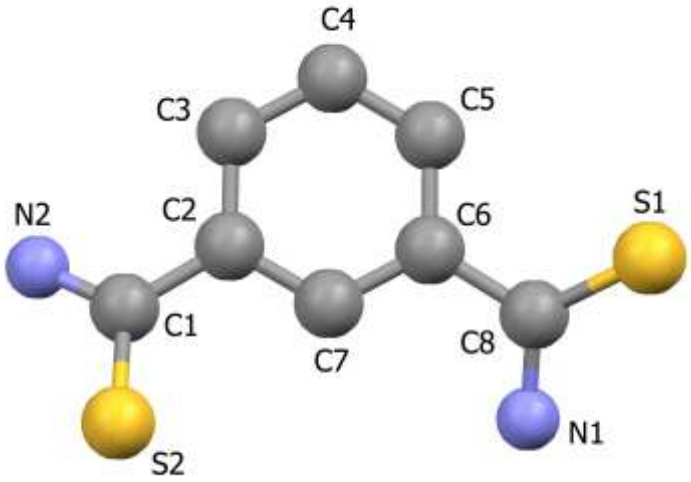

Fig. S9. Drawing of **m-dtab** based on X-ray structure (hydrogen atoms omitted for clarity).

Table S1. Electronic spectra of compounds **m-dtab**, **1 – 3** in solid state.

Compound [a]	Chromofore	Transitions (cm^{-1})	Assignment	Ref
m-dtab		21700; 23500; 25000; 27000, 31000 [b]		this work
1	CoS_2Cl_2	13900; 15300; 16300	$^4A_2(F) \rightarrow {}^4T_1(P)$	this work
		25000	CT	
2	CoS_2Br_2	13400; 14700; 15400	$^4A_2(F) \rightarrow {}^4T_1(P)$	this work
		25000	CT	
3	NiS_4Br_2	13100	$^3B_{1g} \rightarrow {}^3B_{2g}$	this work
		20200	$^3B_{1g} \rightarrow ({}^3E_g + {}^3A_{2g})$	
		25800	$^3B_{1g} \rightarrow ({}^3E_g(P) + {}^3A_{2g}(P)) + CT$	
$Ni(tc)Cl_2$	NiS_4Cl_2	11110, 16950, 29140		16
$Ni(tc)Br_2$	NiS_4Br_2	10990, 16950, 29140		16
$Ni(bme)Br_2$	NiS_4Br_2	10200, 16100, 25000(sh)		17

[a] tc = 1,4,8,11-tetrathiacyclotetradecane, bme = 1,2-bis(*o*-methylthiophenylthio)ethane;

[b] Based on deconvolution using 5 gaussians, $R^2 = 0.99993$ (5^{th} peak is out of spectrum range).

Table S2. *J* values, calculated for exchange interactions through different exchange pathways in the particles, modeling the structure of **1**, by different functionals (for Hamiltonian $H = -2J\sum S_1 S_2$).

Functional	Basis	Pathway[a]	$E_{HS} - E_{BS}$, cm^{-1}	J_1,[b] cm^{-1}	J_2,[b] cm^{-1}	J_3,[b] cm^{-1}
BP	def2-SVP	Co-(m-dtab)-Co	0.823	–0.09	–0.07	–0.09
		π-stacking	2.612	–0.29	–0.22	–0.29
		H-bond	0.019	0	0	0
	def2-TZVP	Co-(m-dtab)-Co	1.898	–0.21	–0.16	–0.21
		π-stacking	2.729	–0.30	–0.23	–0.30
		H-bond	-0.212	0.02	0.02	0.02
TPSS	def2-SVP	Co-(m-dtab)-Co	1.511	–0.17	–0.13	–0.17
		π-stacking	1.999	–0.22	–0.17	–0.22
		H-bond	0.285	–0.03	–0.02	–0.03
	def2-TZVP	Co–(m–dtab)–Co	2.028	–0.23	–0.17	–0.23
		π-stacking	2.634	–0.29	–0.22	–0.29
		H-bond	0.194	–0.02	–0.02	–0.02
B3LYP	def2-SVP	Co–(m–dtab)–Co	0.557	–0.06	–0.05	–0.06
		π-stacking	1.071	–0.12	–0.09	–0.12
		H-bond	0.186	-0.02	-0.02	-0.02
	def2-TZVP	Co–(m–dtab)–Co	0.662	–0.07	–0.06	–0.07
		π-stacking	–	–	–	–
		H-bond	0.172	–0.02	–0.01	–0.02

[a] exchange pathways are described in the text and shown on Fig. S5.

[b] J_1, J_2 and J_3 refer to different schemes of J calculation using HS - BS gap: J_1 – after

Ginsberg, Noodleman and Davidson ($J_1 = -(E_{HS} - E_{BS})/S^2_{max}$));[18] J_2 – after Bencini and Gatteschi ($J_2 = -(E_{HS} - E_{BS})/(S_{max}(S_{max}+1))$);[19] J_3 – after Yamaguchi, Takahara, Fueno and Soda ($J_3 = -(E_{HS} - E_{BS})/(\langle S^2_{HS}\rangle - \langle S^2_{BS}\rangle)$))[20]

Table S3. *J* values, calculated for exchange interactions through different exchange pathways in the particles, modeling the structure of **2**, by BP functional (for Hamiltonian $H = -2J\sum S_1 S_2$).

Functional	Basis	Pathway[a]	$E_{HS} - E_{BS}$, cm^{-1}	J_1,[b] cm^{-1}	J_2,[b] cm^{-1}	J_3,[b] cm^{-1}
BP	def2-SVP	Co–(m–dtab)–Co	1.045	–0.12	–0.09	–0.12
		π-stacking	2.632	–0.29	–0.22	–0.29
		H-bond	–0.206	0.02	0.02	0.02
	def2-TZVP	Co–(m–dtab)–Co	1.849	–0.21	–0.15	–0.21
		π-stacking	2.996	–0.33	–0.25	–0.33
		H-bond	–0.668	0.07	0.06	0.07

[a] exchange pathways are described in the text and shown on Fig. S5.

[b] J_1, J_2 and J_3 refer to different schemes of J calculation using HS - BS gap: J_1 – after Ginsberg, Noodleman and Davidson ($J_1 = -(E_{HS} - E_{BS})/S^2_{max}$));[18] J_2 – after Bencini and Gatteschi ($J_2 = -(E_{HS} - E_{BS})/(S_{max}(S_{max}+1))$);[19] J_3 – after Yamaguchi, Takahara, Fueno and Soda ($J_3 = -(E_{HS} - E_{BS})/(\langle S^2_{HS}\rangle - \langle S^2_{BS}\rangle)$))[20]

Table S4. Comparison of experimental and calculated bond lengths in **m-dtab**.

Bond	X-ray structure determination	Calculation	Difference between experiment and calculation
S2–C1	1.678(3)	1.658	0.020
S1–C8	1.673(3)	1.657	0.016
N1–C8	1.319(3)	1.347	–0.028
N2–C1	1.320(3)	1.348	–0.028
C1–C2	1.481(3)	1.489	–0.008
C2–C3	1.392(3)	1.398	–0.006
C2–C7	1.394(3)	1.396	–0.002
C3–C4	1.383(4)	1.391	–0.008
C4–C5	1.382(4)	1.385	–0.003
C5–C6	1.389(3)	1.399	–0.010
C6–C7	1.390(3)	1.394	–0.004
C6–C8	1.491(3)	1.491	0.000

Table S5. Calculated Mayer's bond orders for model particles – fragments of coordination polymers **1** and Co(m-phthalateH)$_2$(Im)$_2$[11] and ligands.

Model particle	Bond		
	Co–X (X = S or O)	X–C (X = S or O)	C–N in thioamide group
Co(m-dtab)$_2$Cl$_2$	0.6505	1.5383	1.3442; 1.3441
Co(m-phthalateH)$_2$(Im)$_2$	0.5042; 0.5282	1.3513; 1.3961	–
m-dtab	–	1.8742; 1.8549	1.2832; 1.2951
m-phthalateH$_2$	–	1.2297; 1.2293	–

References for Supporting materials

1. (*a*) A. D. Becke, *J. Chem. Phys.*, 1993, **98**, 5648; (*b*) P. J. Stephens, F. J. Devlin, C. F. Chabalowski and M.J. Frisch, *J. Phys. Chem.*, 1994, **98**, 11623; (*c*) A. D. Becke, *Phys. Rev. A.*, 1988, **38**, 3098.
2. C. Lee, W. Yang and R. G. Parr, *Phys. Rev. B.*, 1988, **37**, 785.
3 S. H. Vosko, L. Wilk and M. Nusair, *Can. J. Phys.*, 1980, **58**, 1200.
4. F. Weigend and R. Ahlrichs, *Phys. Chem. Chem. Phys.*, 2005, **7**, 3297.
5. ftp://ftp.chemie.uni-karlsruhe.de/pub/basen
6. (*a*) R. A. Kendall and H. A. Früchtl, *Theor. Chim. Acta*, 1997, **97**, 158; (*b*) F. Neese, *J. Comp. Chem.*, 2003, **24**, 1740.
7. F. Neese, F. Wennmohs, A. Hansen and U. Becker, *Chem. Phys.*, 2009, **356**, 98.
8. C.-K. Skylaris, L. Gagliardi, N. C. Handy, A. G. Ioannou, S. Spencer and A. Willetts, *J. Mol. Struct. (Theorchem)*, 2000, **501-502**, 229**.**
9. (*a*) V. I. Lebedev, *Zh. Vychisl. Mat. Fiz.*, 1975, **15**, 48; (*b*) V. I. Lebedev, *Zh. Vychisl. Mat. Fiz.*, 1976, **16**, 293; (*c*) V. I. Levedev, D. N. Laikov, *Doklady Mathematics*, 1999, **59**, 477; (*d*) V. I. Lebedev and A. L. Skorokhodov, *Sov. Phys.-Dokl.*, 1992, **45**, 587; (*e*) M. Eden and M. H. Levitt, *J. Magn. Res.*, 1998, **132**, 220.
10. S. Grimme, J. Antony, S. Ehrlich and H. Krieg, *J. Chem. Phys.*, 2010, **132**, 154104.
11. J.-F. Song, Y. Chen, Z.-G. Li, R.-S. Zhou, X.-Y. Xu and J.-Q. Xu, *J. Mol. Struct.*, 2007, **842**, 125.
12. Avogadro: an open-source molecular builder and visualization tool. Version 1.00. http://avogadro.openmolecules.net/
13. (*a*) I. Mayer, *Chem. Phys. Lett.*, 1983, **97**, 270; (*b*) I. Mayer, *Int. J. Quant. Chem*, 1984, **26**, 151; (*c*) I. Mayer, *Theor. Chim. Acta*, 1985, **67**, 315.
14. J. P. Perdew, *Phys. Rev. B*, 1986, **33**, 8822.

15. J. Tao, J. P. Perdew, V. N. Staroverov and G. E. Scuseria, *Phys. Rev. Lett.*, 2003, 91, 146401.

16. W. Rosen and D. H. Busch, *J. Chem. Soc. D, Chem. Comm.*, 1969, 148.

17. W. Levason, Ch. A. McAuliffe and S. G. Murray, *J. Chem. Soc., Dalton Trans.*, 1975, 1566.

18. (*a*) A. P. Ginsberg, *J. Am. Chem. Soc.*, 1980, **102**, 111; (*b*) L. Noodleman, *J. Chem. Phys.*, 1981, **74**, 5737; (*c*) L. Noodleman and E. R. Davidson, *Chem. Phys.*, 1985, **109**, 131.

19. A. Bencini and D. Gatteschi, *J. Am. Chem. Soc.*, 1980, **108**, 5763.

20. (*a*) K. Yamaguchi, Y. Takahara and T. Fueno in: V.H. Smith (Ed.), *Applied Quantum Chemistry,* Reidel, Dordrecht, 1986, p. 155; (*b*) T. Soda, Y. Kitagawa, T. Onishi, Y. Takano, Y. Shigeta, H. Nagao, Y. Yoshioka and K. Yamaguchi, *Chem. Phys. Lett.*, 2000, 319, 223.